JAERI-M
88-040

AC LOSS TIME CONSTANT MEASUREMENTS ON Nb_3Al AND NbTi MULTIFILAMENTARY SUPERCONDUCTORS

March 1988

T. A. PAINTER*

日 本 原 子 力 研 究 所
Japan Atomic Energy Research Institute

JAERI-Mレポートは，日本原子力研究所が不定期に公刊している研究報告書です。
入手の問合わせは，日本原子力研究所技術情報部情報資料課（〒319-11 茨城県那珂郡東海村）あて，お申しこしください。なお，このほかに財団法人原子力弘済会資料センター（〒319-11 茨城県那珂郡東海村日本原子力研究所内）で複写による実費領布をおこなっております。

JAERI-M reports are issued irregularly.
Inquiries about availability of the reports should be addressed to Information Division Department of Technical Information, Japan Atomic Energy Research Institute, Tokaimura, Naka-gun, Ibaraki-ken 319-11, Japan.

編集兼発行　日本原子力研究所
印　　刷　日青工業株式会社

JAERI-M 88-040

AC Loss time constant measurements on Nb_3Al and NbTi Multifilamentary Superconductors

T.A. PAINTER*

Department of Thermonuclear Fusion Research
Naka Fusion Research Establishment
Japan Atomic Energy Research Institute
Naka-Machi, Naka-Gun, Ibaraki-ken

(Received February 1, 1988)

The AC loss time constant is a previously uninvestigated property of Nb_3Al, a superconductor which, with recent technological developments, shows some advantages over the more commonly used superconductors, NbTi and Nb_3Sn. Four Nb_3Al samples with varying twist pitches and one NbTi sample are inductively measured for their AC loss time constants. The measured time constants are compared to the theoretical time constant limits imposed by the limits of the transverse resistivity found by Carr [5] and to the theoretical time constants found using the Bean Model as well as to each other. The measured time constants of the Nb_3Al samples fall approximately halfway between the theoretical time constant limits, and the measured time constants of the NbTi sample is close to the theoretical lower time constant limit. The Bean Model adequately accounts for the variance of the permeability of the Nb_3Al superconductor in a background magnetic field. Finally, the measured time constant values of the Nb_3Al samples vary approximately according to the square of their twist pitch.

Keywords: Nb_3Al, NbTi, Superconductors, AC Loss Time Constant

---

* Massachusetts Institute of Technology

Nb_3Al とNbTi 多芯線の交流損失時定数の測定

日本原子力研究所那珂研究所核融合研究部
T. A. PAINTER*

（ 1988年2月1日受理 ）

Nb_3Al 多芯線の交流損失時定数について研究した。実験は，ツイスト・ピッチの異なる4個のNb_3Al 試料とそれらの比較として1個のNbTi 試料について行った。これらの実験結果は，Carr により提示された横方向抵抗率に関する2つの上下極限理論と比較検討した。Nb_3Al の測定値は2つの極限の丁度中間になり，又，NbTi は下限理論に近いことが解った。又，低磁界側でのピーク効果は，Bean Model を用い透磁率の変化を考慮することにより定性的に説明出来ることが解った。

那珂研究所：〒311-01　茨城県那珂郡那珂町大字向山801−1
＊　米国マサチューセッツ工科大学

Contents

目　　次

1. Introduction

Superconductivity was first observed by Kammerlingh Onnes in 1911 while he was investigating the properties of various metals at a liquid-helium temperatures. He found that below a certain critical temperature, the electrical resistance of mercury wire suddenly decreased to zero. Soon after this discovery, he also found that above a critical magnetic field (in Onnes' case, approximately 1/20 Tesla) [1], the superconducting metal would return to its normal electrically resistive state. Although Onnes discovered an amazing new phenomenon, he was also immediately introduced to its severe limitations that hindered its practical use. Luckily, researchers believed that superconductors could be developed to overcome these limitations and enter the realm of practicality.

From Onnes' discovery until the present, there has been much success in the superconducting field. Many new superconducting materials have been developed, and two of these materials, NbTi and Nb_3Sn, have performed very well in many concrete applications. Some of these applications have been a) research magnets, b) high energy physics, c) magnetically levitated trains, d) energy storage, and e) thermonuclear fusion [1], which is now achievable through the development of superconducting magnets that are capable of producing the high magnetic fields required for fusion.

Although NbTi and Nb_3Sn are the present workhorses of the superconducting industry, many promising superconducting materials are still being investigated. One of these materials, Nb3Al, further elevates the limits of superconductivity in terms of its critical magnetic field while remaining practical in its other superconducting properties. This paper focuses on a previously uninvestigated property of Nb3Al, the time constant of its AC coupling loss.

1.1 Work Objective

The work objective of this study is to investigate the AC coupling loss time constants of four multifilamentary Nb3Al superconducting samples and one multifilamentary NbTi sample. First, the experimental set-up is arranged and the time constants are experimentally measured for all the superconducting samples. Second, the results of the testing are organized and recorded. Third, the results are discussed and compared to the theoretical time constant values and to each other.

Finally, suggestions are made for further areas of research of the multifilamentary Nb_3Al superconductor.

1.2 Why Niobium$_3$ Aluminum ?

Nb_3Al holds two significant advantages over the more commonly used materials, NbTi and Nb_3Sn: first, it has a higher critical magnetic field, and second, it maintains its high critical magnetic field when stressed. Fig. 1 shows a comparison of the critical magnetic fields as a function of temperature for Nb_3Al, Nb_3Sn, and NbTi. Nb_3Al has a critical magnetic field at zero kelvin which is approximately 50% higher than the critical magnetic field of Nb_3Sn and approximately 140% higher than the critical magnetic field of NbTi. Fig. 2 [2] shows a comparison of the deterioration in the normalized critical magnetic fields of various superconductors as the superconductor is strained. Nb_3Al has the least deterioration of all the superconductors shown, and furthermore, at 0.4% strain, the normalized critical magnetic field of Nb_3Al deteriorates only 20% as much as Nb_3Sn.

Both of these advantages make Nb_3Al an excellent candidate for use as a superconducting material in a fusion power generator. In a fusion power generator, equation 1 and 2 apply, where P is the power output, D is the diameter of the superconducting magnet that confines the hot

$$P \sim (D)^2(B)^4 \quad (1)$$

$$S \sim (D)(B) \quad (2)$$

plasma, B is the magnetic field produced, and S is the stress in the magnet. According to equation 1, the power output can be increased by increasing D. But by increasing D, the stress in the superconducting magnet is also increased. The increased stress will, in turn, decrease the critical magnetic field of the superconducting magnet as shown in Fig. 2, and the decreased critical magnetic field will cause a decrease in the power output, which acts to negate the gain received by increasing the diameter of the superconducting magnet. In the case of Nb_3Al, the critical magnetic field is initially higher than the two commonly used superconductors, Nb_3Sn and NbTi, which have already been applied in fusion power research [3], and also, its critical magnetic field does not deteriorate as rapidly as other superconducting materials as the strain increases. Both of these properties make Nb_3Al an ideal candidate for

a superconducting material in a fusion power generator, although the Nb_3Al superconductor does have a disadvantage.

The reason Nb_3Al has not been used in fusion power research is its low critical current density as compared to Nb_3Sn. With the development of oxygen free Niobium and Aluminum within the past several years, Nb_3Al has begun to realize its potential for high critical current densities, and developments are still being made in this direction. In particular, fabrication techniques are being developed in order to create Nb_3Al with none of its associated nonsuperconducting impurities, Nb_2Al and $NbAl_3$. For this reason, Nb_3Al does not yet exist as a commercial wire. Because of its low critical current densities, a Nb_3Al superconducting magnet presently would require more volume to attain the high magnetic fields required by a fusion power generator. This adds to the size and the cost of fusion power production. But through further research, the low critical current of Nb_3Al will be increased in a few years to competitive values.

1.3 AC Loss

The AC loss in a multifilamentary superconductor is the electrical energy loss caused by a changing external magnetic field. The change in the magnetic field causes the superconductor to return to its normal electrically resistive state which then combines with the current to generate a power loss. This power loss adds to the inefficiency of fusion power generation, where changing magnetic fields are required. For this reason AC loss is critical in the design of a fusion power generator.

There are three areas of AC loss in superconducting materials: 1) hysteresis loss, 2) eddy current loss, and 3) coupling loss. Hysteresis loss is a property of the superconducting material and the eddy current loss is a property of the stabilizing matrix. For a given superconducting material and matrix, only the coupling loss can be reduced. This can be accomplished by varying the geometry and twist pitch of the superconducting filaments. Luckily, the losses which can not be controlled, hysteresis and eddy current, normally account for the smaller percentage of the total AC losses. In a fusion power generator, the coupling loss can exceed 90% of the total AC losses of the superconductor.

1.4 The Time Constant of the AC Coupling Loss in a Multifilamentary Superconductor

The time constant of the AC coupling loss in the multifilamentary superconductor is an important parameter for comparing the AC coupling loss in different types of superconductors. The time constant of the AC coupling loss is found by measuring the decay of the current generated between the superconducting filaments when a nearly instant external magnetic field change occurs. These measurements, which have been developed at The Japan Atomic Energy Research Institute (JAERI) [4], are useful when developing a superconductor for a fusion power generator, where the losses caused by the changing magnetic fields are critical to the feasibility of fusion power.

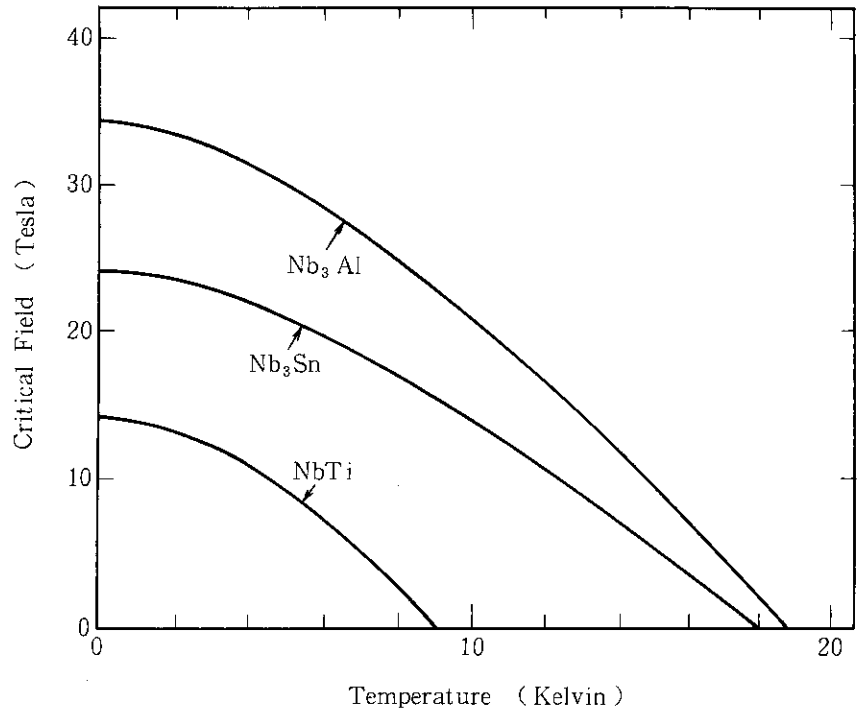

Fig. 1 Nb_3Al has a higher critical magnetic field than the two types of superconducting materials, Nb_3Sn and NbTi, which has been commonly used in many superconducting applications.

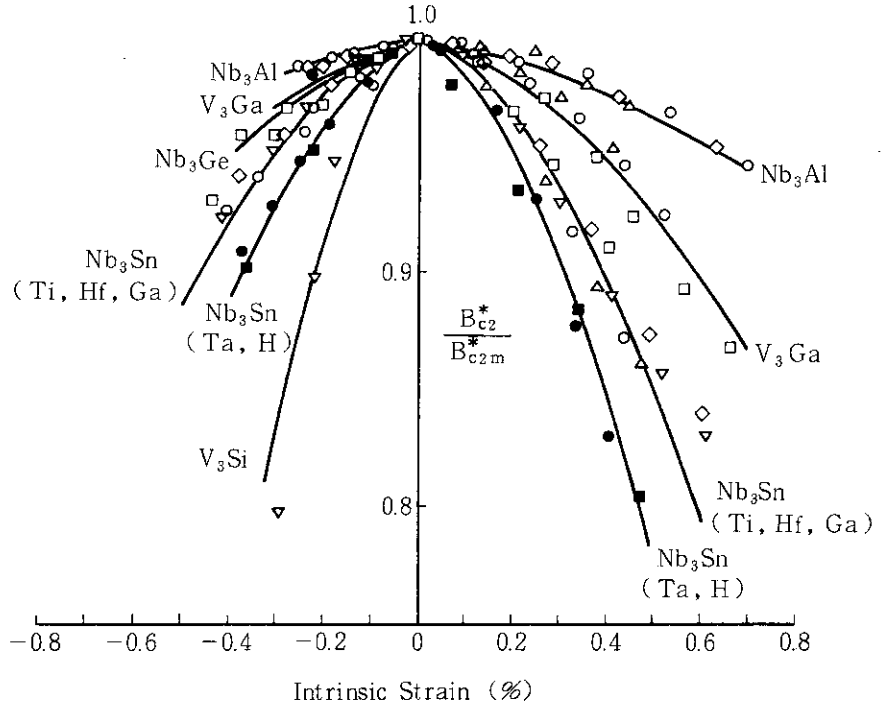

Fig. 2 The critical magnetic field of Nb3Al deteriorates very little when stressed.

2. Experiment

The focus of this study was to measure and investigate the magnetic field dependence of the time constants of two types of multifilament superconductor samples. These time constant experiments are described in the following two sections. The first section describes the two types of superconducting samples investigated, and the second section describes the experimental technique used to measure the time constants.

2.1 Types of Superconducting Samples Under Investigation

Two types of superconducting samples were investigated in this study, NbTi and Nb_3Al. The cross-sections of these samples are shown in Fig. 3, and the specifications of the samples are given in Table 1. Only one sample of the NbTi type was investigated, but four differing samples of the Nb_3Al type were investigated. The Nb_3Al samples were manufactured using the jelly roll method by Sumitomo Electric Industries, LTD, and the distinctive parameter was the twist pitch, which was 10 mm, 15 mm, 30 mm, and 40 mm for each sample, respectively.

2.2 Time Constant Measurement Technique

An inductive method was used to measure the time constants of the superconducting samples. In this method, three coils were strategically placed so that their mutual induction could be used to first initiate a current in the superconducting sample coil and then measure its decay. This method is divided into three sections in order to provide an easy explanation. The first section, physical arrangement of the coils, explains the positioning and purpose of each of the three coils. The second section, experimental procedure, explains in detail the operation of each coil and the method of procuring a time constant measurement. The third section, calculation of the time constant, explains how a time constant was derived from the experimental measurement.

2.2.1 Physical Arrangement of the Coils

The following coil arrangement was used to inductively measure the time constants of the superconducting samples. The superconducting sample coil was first wound onto a solid cylinder. A "pickup" coil was then wound onto the outside of the sample coil in order to inductively

measure any current change in the sample coil. This configuration of sample coil and pickup coil was then placed inside a third coil, the pulse coil, which was used to inductively generate a current in the sample coil. This set of three coils was finally placed inside of a permanent dewar which contained a superconducting magnet used to generate a background magnetic field. See Fig. 4 for a picture of the experimental probe and Fig. 5 for a schematic drawing of the coil arrangement. Table 2 lists the specifications of each coil.

2.2.2 Experimental Procedure

The following experimental procedure was used to obtain each time constant measurement. The pulse coil was supplied with a ramped pulse of current that increased at a constant rate of 0.35 amps per millisecond. After 200 milliseconds, the current supply to the pulse coil was automatically disengaged, and the current in the pulse coil rapidly decayed with the relatively small time constant of 50 μS. This sharp drop in current produced a sudden magnetic field change of approximately 0.2 Tesla across the sample coil. Through mutual inductance, the sudden magnetic field change caused a voltage and current in the sample coil. The induced sample coil current then decayed at its own rate. This decay produced a second, slower magnetic field change which, through mutual inductance, caused a voltage in the pickup coil that paralleled the decay rate of the current in the sample coil. See Fig. 6 for an illustration of the pulse coil current and pickup coil voltage during a time constant measurement. After each time constant measurement, the background magnetic field was increased, and the above procedure was repeated to measure the next time constant. See Fig. 7 for a schematic of the experimental setup.

2.2.3 Calculation of the Time Constant

The time constant was derived from the experimental measurement in the following manner. During the decay of the sample coil current, the pickup coil voltage was recorded on an oscilliscope, and then photographed. Fig. 8 shows a typical photograph of an oscilliscope recording. Data points from this photograph were then plotted on semilog paper and a straight line was drawn. Fig. 9 shows the semilog plot of the oscilliscope photograph in Fig. 8. The time constant was drawn from the

semilog plot by measuring on the x-axis the amount of time required for the pickup coil voltage to reach 36.7 percent of its y-intercept value.

Table 1 Specification of the two types of superconductors under investigation

NIOBIUM TITANIUM

Wire Diameter	0.9 mm
Number of Filaments	931
Filament Diameter	21 m
Copper Ratio	0.98
Twist Pitch	32 mm
Thickness of Insulation	33 m

NIOBIUM$_3$ ALUMINUM

Wire Diameter	1.16 mm
Number of Filaments	91
Outer Diameter of Filaments	70 m
Inner Diameter of Filaments	28 m
Copper Ratio	2.6
Twist Pitches	10, 15, 30, and
No Insulation	40 mm, and infinity

Table 2 Specifications of the coils used for the time constant measurements

	Pulse Coil	Sample Coil	Pickup Coil
Length (mm)	100	50	10
Inside Diameter (mm)	30	20	22 *
Wire Diameter (mm)	0.45	1.0 *	0.1
Number of Layers	1	1	2
Number of Turns	214	47 *	170 *
Inductance (μH)	375 *	17 *	390 *
Wire Material	Cu	NbTi Nb_3Al	Cu

* Approximate value

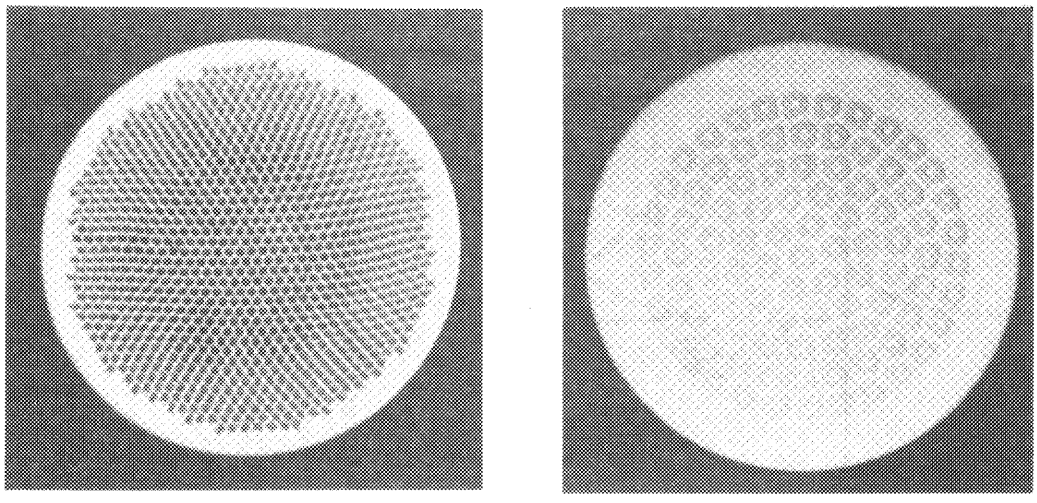

NbTi Nb_3Al

Fig. 3 The experimental probe used to measure the AC loss time constants of Nb_3Al and NbTi.

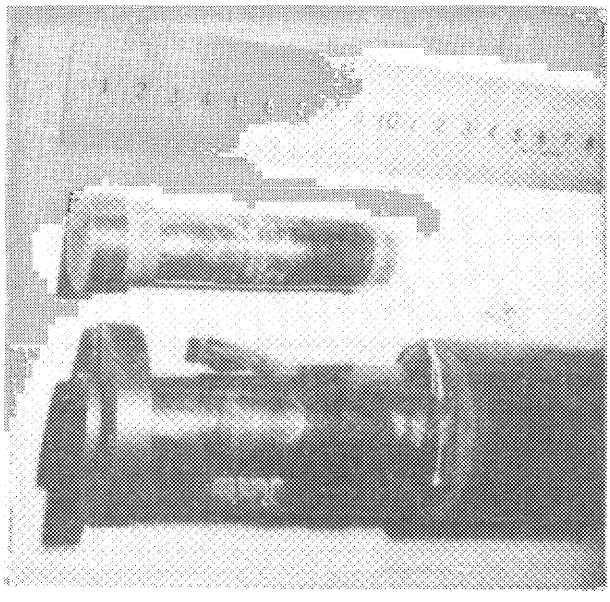

Fig. 4 Cross-sectional photographs of the two types of superconducting wire under investigation, NbTi and Nb_3Al.

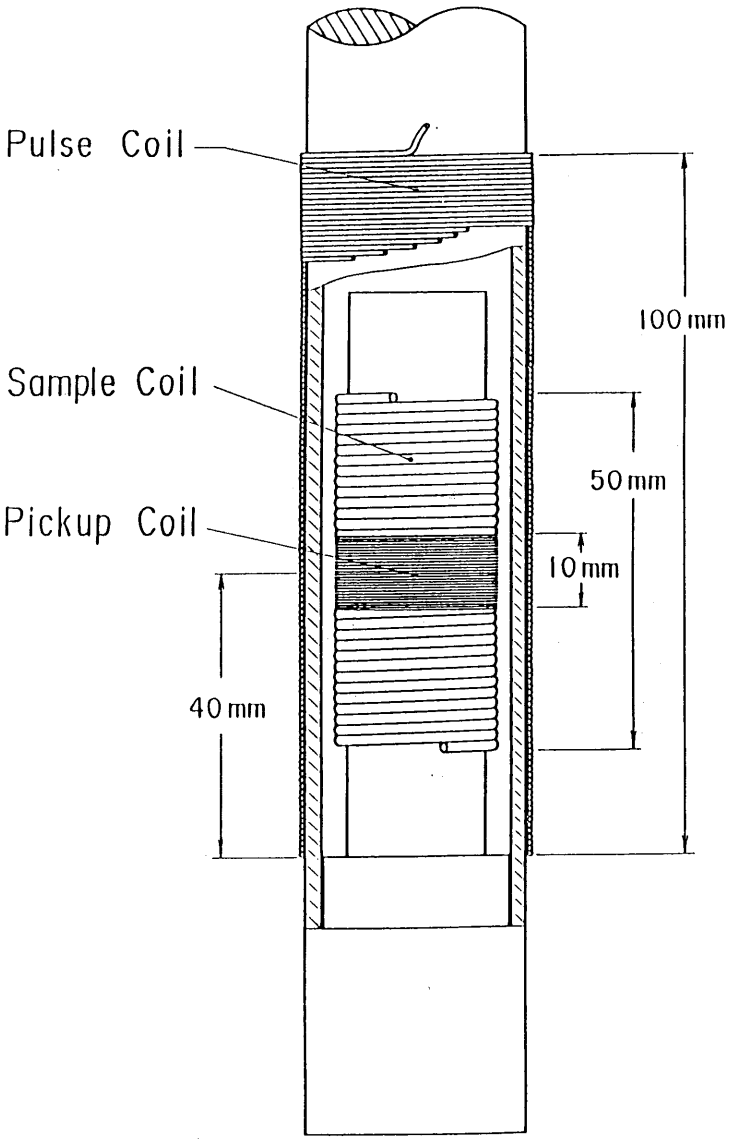

Fig. 5 The relative size and location of the coils used for the time constant measurements.

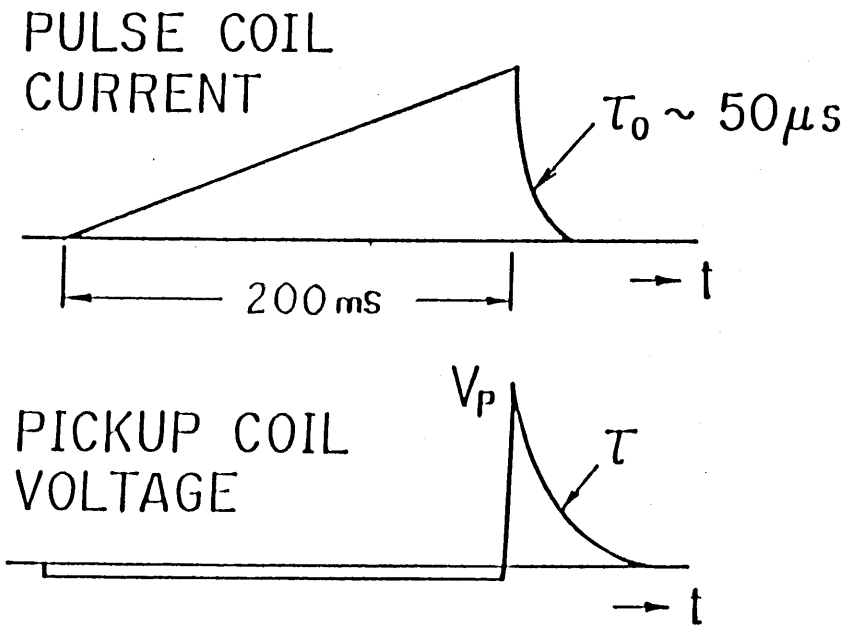

Fig. 6 The pulse coil current and pickup coil voltage during a time constant measurement. T_f is calculated from the decay curve of the pickup coil voltage.

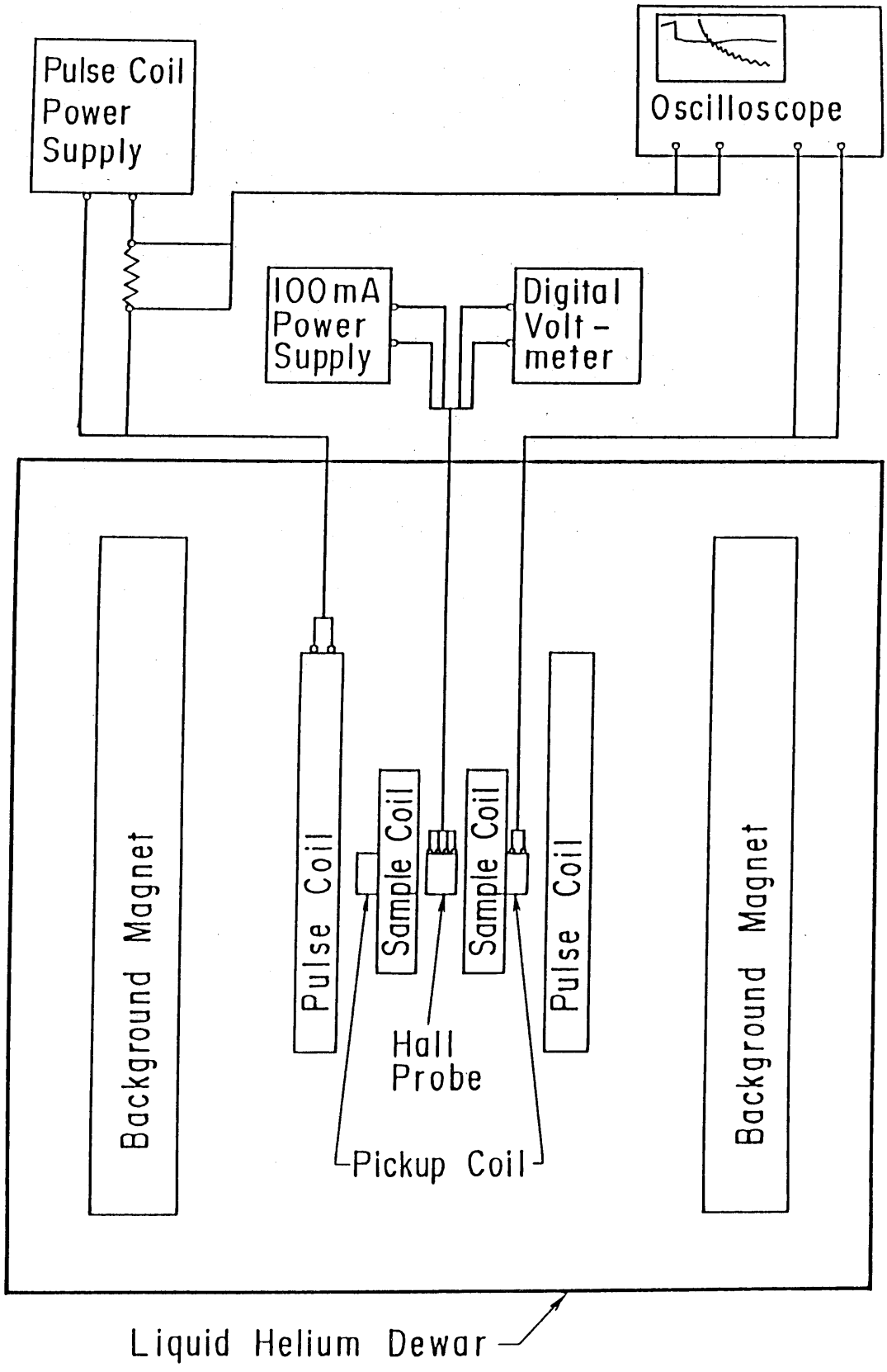

Fig. 7 An electrical schematic of the experimental setup used for the time constant measurements.

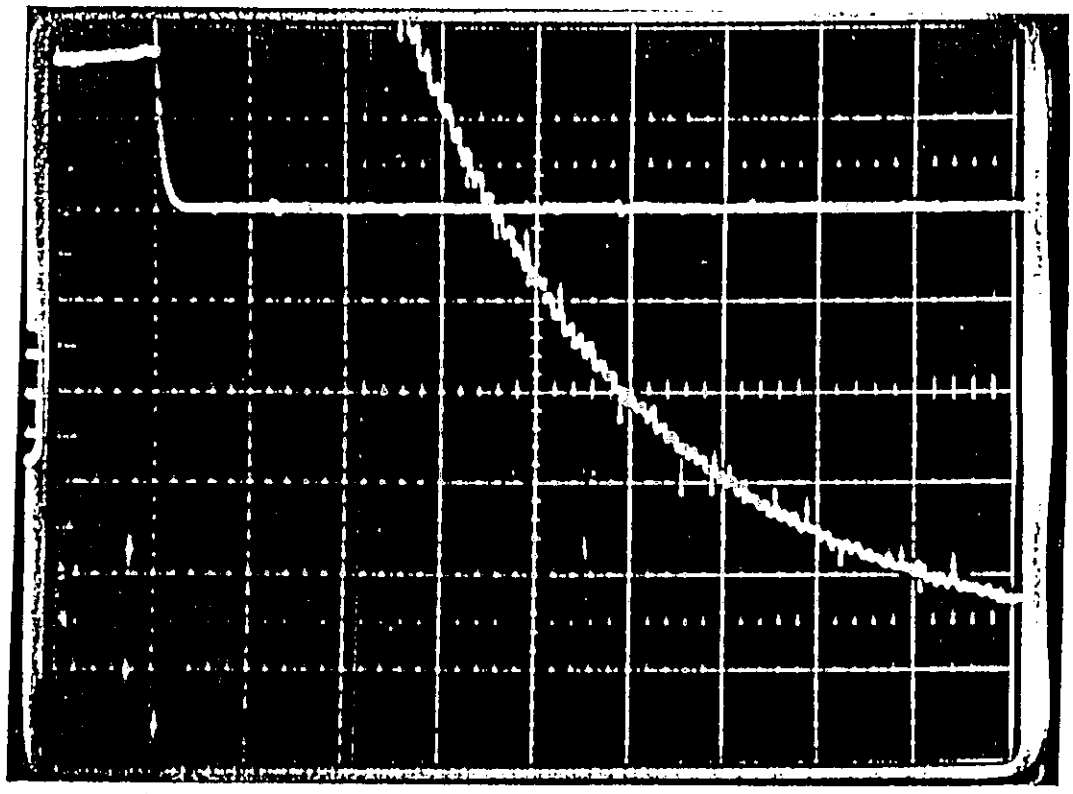

Fig. 8 A typical oscilliscope recording of the pickup coil voltage during a time constant measurement.

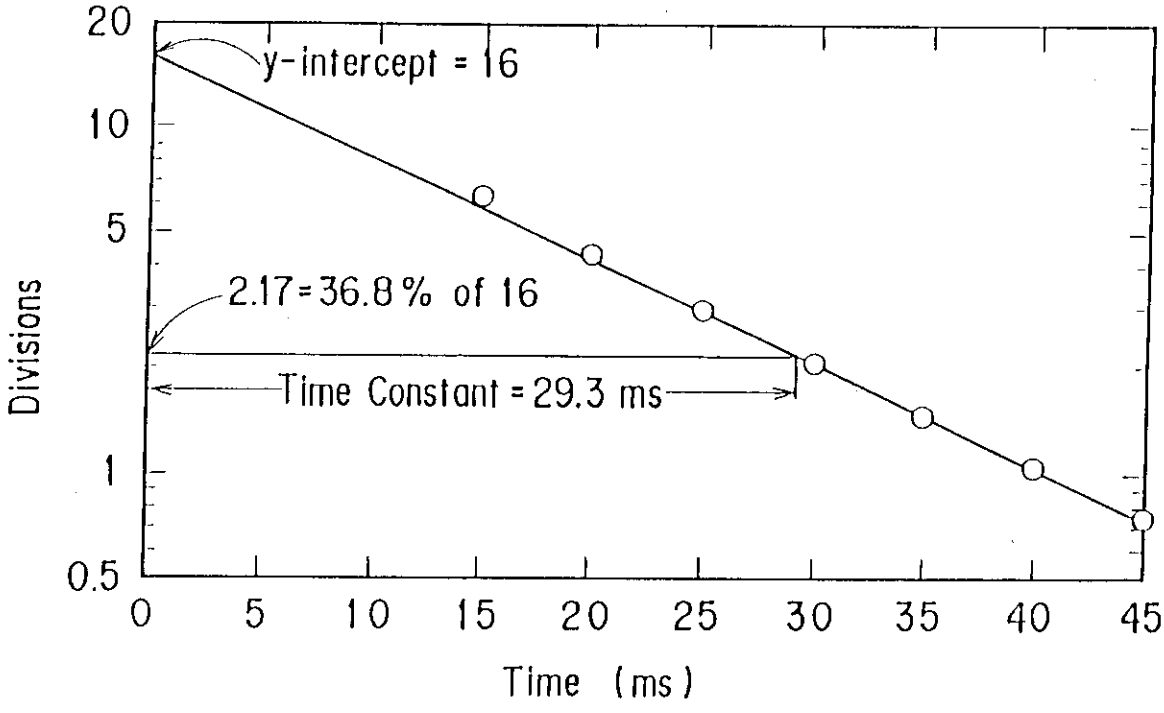

Fig. 9 The semilog plot used to procure a time constant from the experimental measurement shown in Fig. 8.

3. Results

The focus of this study was to measure and investigate the background magnetic field dependence of the time constants of two types of multifilament superconducting materials, NbTi and Nb_3Al. Each superconducting sample was tested at least one time, and for the first test of each sample the measurements began in a background magnetic field of approximately 0.4 tesla. The measurements could not begin in a background magnetic field of zero tesla because of a residual magnetic field retained by the magnet after the current of the background magnet was returned to zero. One way to counteract this affect was to warm up the magnet from 4.2 Kelvin, the measuring temperature, to approximately 20 Kelvin, at which point the background magnet would lose its residual field. This was done before the second test of the 10 mm and 30 mm twist pitch samples of Nb_3Al in order to inspect in finer detail the time constant dependency at low fields. Also, zero background magnetic field measurements were conducted on the remaining samples in a different dewar with no background magnet in order to avoid the residual magnetic field affects. In all cases, the time constants were measured in increasingly higher magnetic fields until the noise during the measurement, which increased as the magnetic field was increased, became too great to obtain a valid reading. The amount of noise also depended on the amount of work going on in the laboratory and the twist pitch of the sample, where a sample with a higher twist pitch tended to generate a measurement with more noise than a sample with a lower twist pitch.

The results of this investigation are divided into two sections. The first section presents the results of the time constant measurements of the Nb_3Al samples, in which four samples with differing twist pitches were tested. The second section presents the results of the time constant measurement of the NbTi sample, in which only one sample was tested.

3.1 The Time Constant Measurements of Niobium$_3$ Aluminum

The time constants of four samples of the Nb_3Al type superconductor were measured. These samples varied only in the twist pitches of their superconducting filaments, which were 10 mm, 15 mm, 30 mm, and 40 mm, respectively. Three of these samples were tested twice and the 40 mm twist pitch sample was tested once. The following four sections present the results of these tests.

3.1.1 The 10 mm Twist Pitch Sample

Figure 10 shows the results of the two tests conducted on the 10 mm twist pitch Nb_3Al sample. The first test measured the time constants in background magnetic fields from 0.41 tesla to 6.0 tesla, and the second test measured in finer detail the time constants in background magnetic fields from zero tesla to 3.0 tesla.

The first test showed a steady decrease in the time constant values, as the background magnetic field was increased with a slight peak in the data occuring at approximately one tesla. The time constant values decreased from a maximum of 21.5 ms at 0.6 tesla to a minimum of 13.0 ms at 6.0 tesla with a slight peak of 20.5 ms occuring between these values at 1.0 tesla.

The second test showed an exponential decrease in the measured time constant values, as the background magnetic field was increased, with two peaks in the data occurring at approximately 0.3 and 1.0 tesla. The time constant values decreased from 27.25 ms at zero tesla to 21.0 ms at 0.09 tesla where the data then sharply rose to its first peak of 28.25 ms at 0.27 tesla. After the first peak, the data decreased sharply to a minimum of 16.5 ms at 0.85 tesla. A second, more rounded peak occurs with a maximum of 18.0 ms at 0.95 tesla, and after the second peak, the data decreased to 12.5 ms at 3.0 tesla.

3.1.2 The 15 mm Twist Pitch Sample

Figure 11 shows the results of the two tests conducted on the 15 mm twist pitch Nb_3Al sample. The first test measured the time constants in background magnetic fields from 0.42 tesla to 8.0 tesla, and the second test measured the time constants from zero tesla to 7.0 tesla.

The first and second test both showed a steady decrease in the time constants as the background magnetic field was increased. In the first test, the time constant values decreased from a maximum of 37.0 ms at 0.42 tesla to a minimum of 11.75 ms at 8.0 tesla. In the second test, the time constant values decreased from 42.0 ms at zero tesla to a minimum of 17.75 ms at 7.0 tesla.

3.1.3 The 30 mm Twist Pitch Sample

Figure 12 shows the results of the two tests conducted on the 30 mm twist pitch Nb_3Al sample. The first test measured the time constants in background magnetic fields from 0.44 tesla to 7.5 tesla, and the second test measured in finer detail the time constants in background magnetic fields from zero tesla to 5.0 tesla.

The first test showed a decrease in the time constant values, as the background magnetic field was increased, with a peak in the data occuring at 3.0 tesla. The time constant values decreased from a maximum of 103 ms at 0.44 tesla to a mininum of 86 ms at 1.6 tesla where the data then rose to a peak of 99 ms at 3.0 tesla. After the peak, the data decreased to a minimum of 64 ms at 6.5 tesla.

The second test showed a decrease in the time constant values, as the background magnetic field was increased, with two peaks in the data occuring at 0.1 tesla and 2.0 tesla. The time constant values began from 144 ms at zero tesla and immediately rose to its first peak of 189 ms at 0.1 tesla. After the first peak, the data decreased sharply to a minimum of 105 ms at 0.5 tesla, and then increased slowly with some fluctuation to a peak of 108 ms at 2.0 tesla. After the second peak, the data decreased to a minimum of 74 ms at 5.0 tesla.

3.1.4 The 40 mm Twist Pitch Sample

Figure 13 shows the results of the test conducted on the 40 mm twist pitch Nb_3Al sample. This test measured the time constants in background magnetic fields from zero tesla to 8.0 tesla, and showed a decrease in the data, as the background magnetic field was increased, with a peak in the data occuring at 2.5 tesla. The time constant values decreased from a maximum of 260 ms at zero tesla to a minimum of 172.5 ms at 0.6 tesla where the data then rose with some fluctuation to a peak of 195.0 ms at 2.5 tesla. After the peak, the data decreased to a minimum of 120.0 ms at 7.5 tesla.

3.2 The Time Constant Measurements of Niobium Titanium

Figure 14 shows the results of the test conducted on the NbTi sample. The test measured the time constants in background magnetic fields from zero tesla to 10.0 tesla. The measured time constant values showed a peak at low background magnetic fields with a maximum time constant of 42.5 ms occuring at both 0.8 and 1.4 tesla. The time constant values began from 25.0 ms at zero tesla, and rose with some fluctuation to the peak mentioned above. After the peak, the time constant values decreased smoothly to 20.5 ms at 8.5 tesla, and then dropped suddenly to a minimum of 8.0 ms at 9.5 tesla.

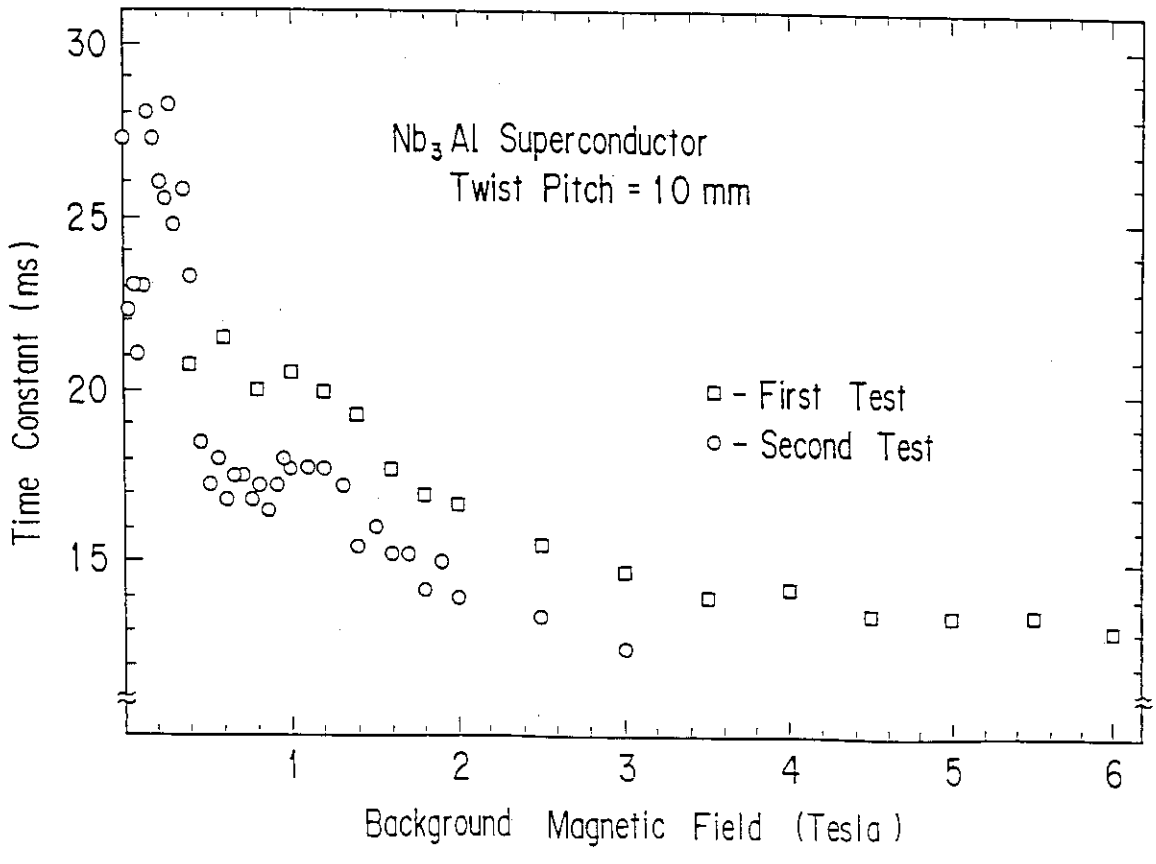

Fig. 10 The test results of the time constant measurements conducted on the Nb3Al superconducting sample coil with a twist pitch of 10 mm.

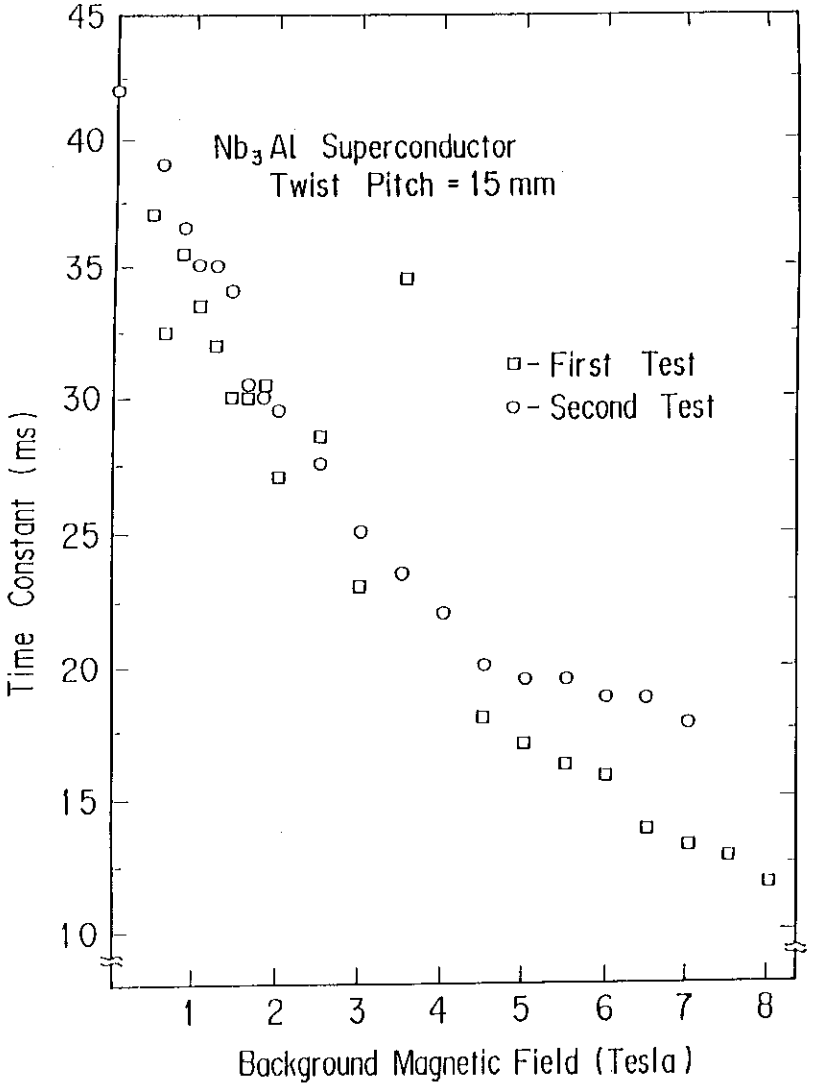

Fig. 11 The test results of the time constant measurements conducted on the Nb_3Al superconducting sample coil with a twist pitch of 15 mm.

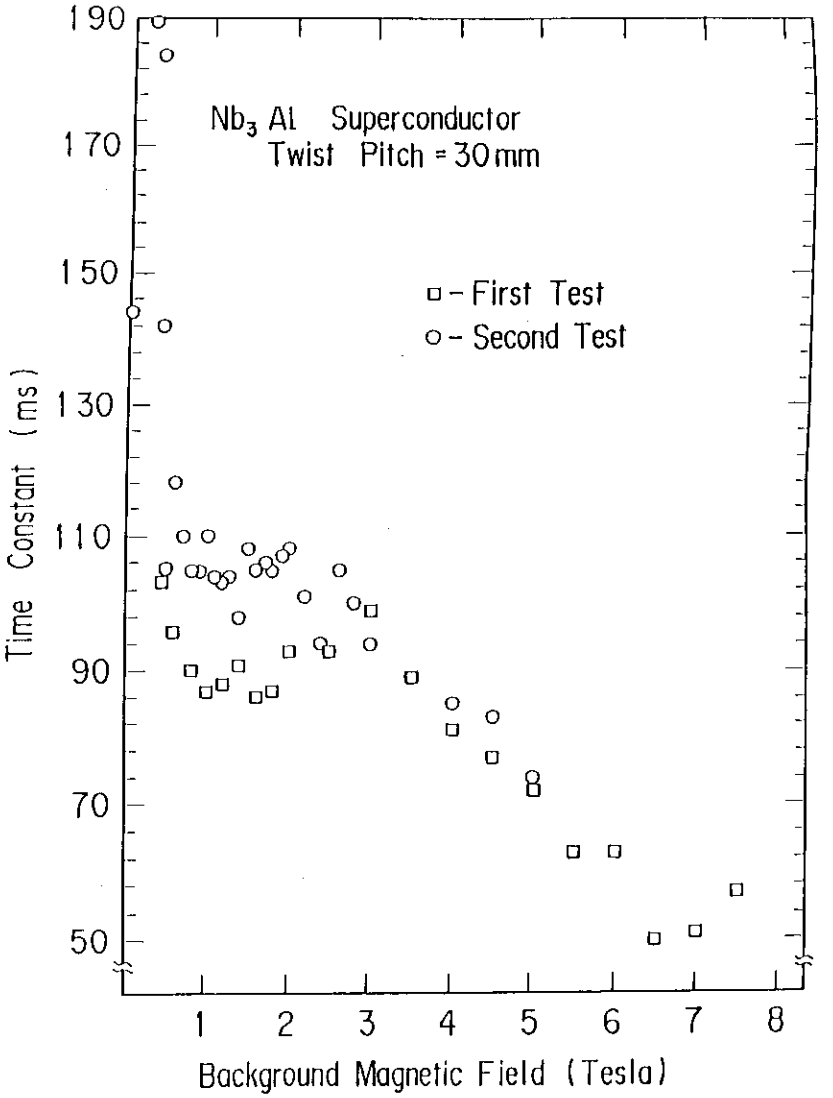

Fig. 12 The test results of the time constant measurements conducted on the Nb_3Al superconducting sample coil with a twist pitch of 30 mm.

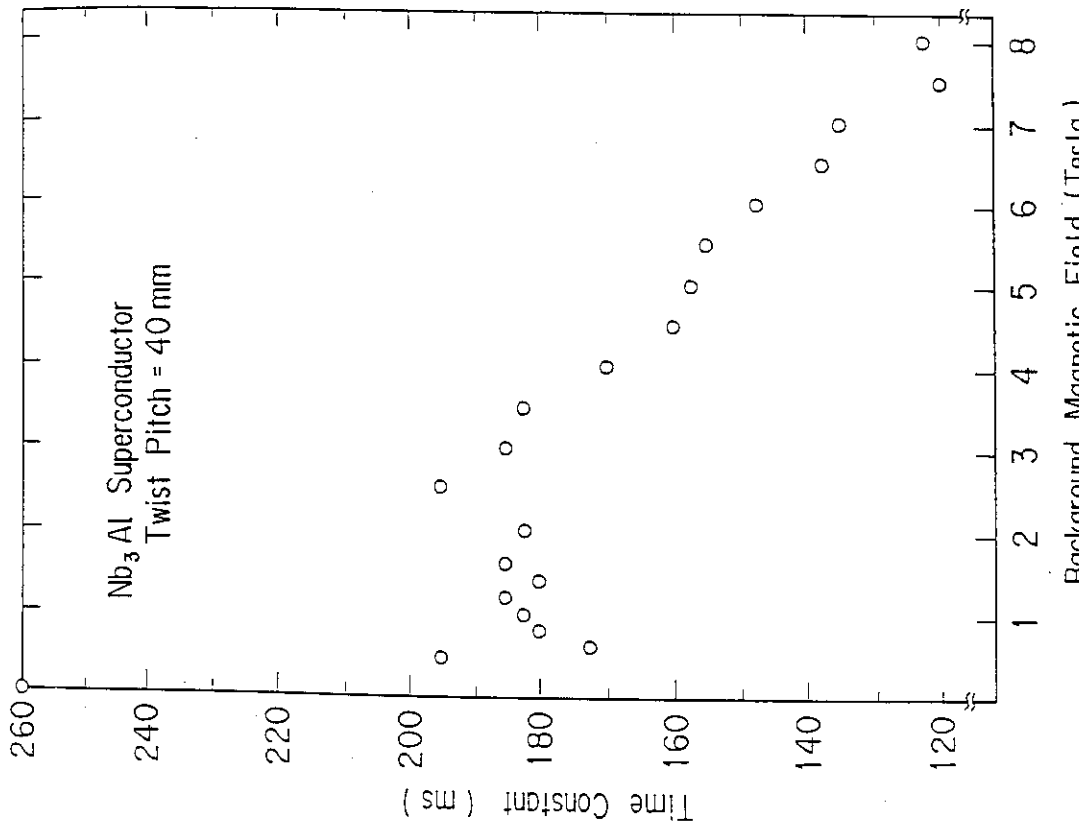

Fig. 13 The test results of the time constant measurements conducted on the Nb_3Al superconducting sample coil with a twist pitch of 40 mm.

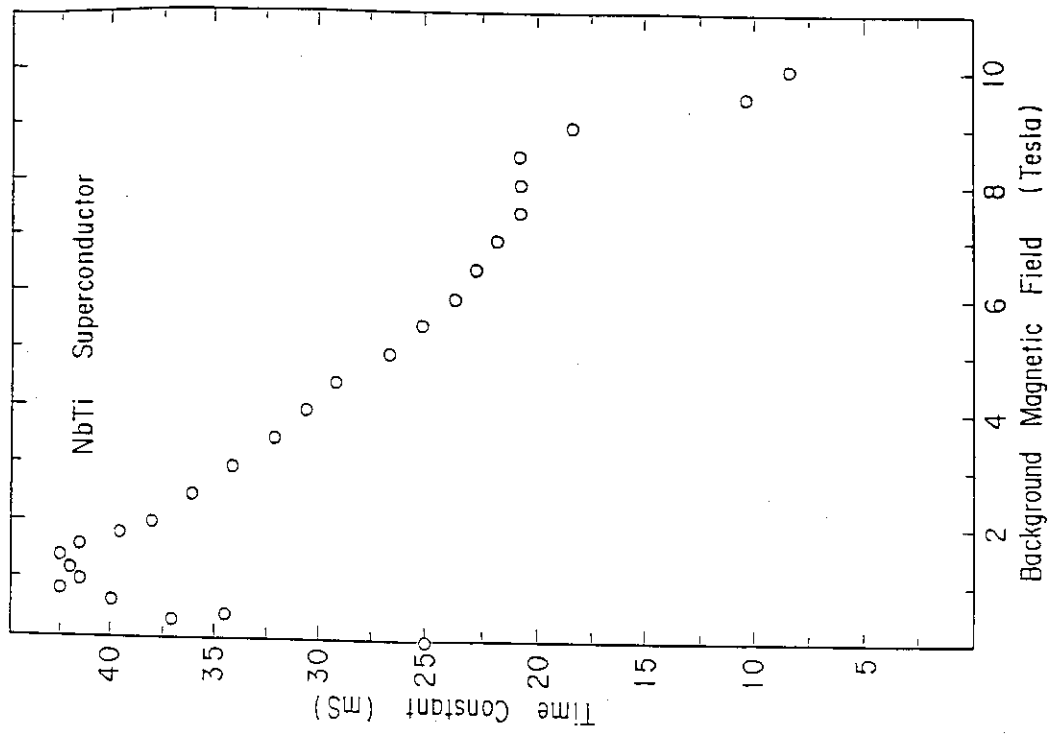

Fig. 14 The test results of the time constant measurements conducted on the NbTi superconducting sample coil

4. Discussion

The following two sections discuss the results of the AC loss time constant measurements. The first section outlines the equations used to obtain the theoretical time constant values, and the second section compares the results of the AC loss time constant measurements with the theoretical values.

4.1 Calculation of the Time Constant of the AC Coupling Loss

The calculation of the time constant of the AC coupling loss in multifilamentary superconductors is given by equation 3 [1],

$$T = (\mu_{ef} L^2)/(8\rho_{et}\pi^2) \tag{3}$$

where L is the twist pitch of the superconducting filaments, μ_{ef} is the effective permeability of the superconducting filaments, and ρ_{et} is the effective transverse resistivity of the superconductor. The parameters μ_{ef} and ρ_{et} depend on the background magnetic field surrounding the superconductor as well as some geometric parameters of the superconductor itself. The following two sections present the calculations used to find μ_{ef} and ρ_{et} as a function of the background magnetic field and geometric parameters of the superconductor.

4.1.1 The Effective Transverse Resistivity

The effective transverse resistivity of a multifilamentary superconductor was found by Carr [5] to fall between the two limits given by equations 4 and 5, where ρ_t is the transverse resistivity of a unit filament, λ is the volume fraction of the superconducting filaments, and P_m is the copper matrix resistivity. Equation 4 is the theoretical

$$\rho_t = \rho_m(1-\lambda)/(1+\lambda) \tag{4}$$

$$\rho_t = \rho_m(1+\lambda)/(1-\lambda) \tag{5}$$

lower of the transverse resistivity when no contact resistance exists between the superconducting filaments and the copper matrix. Equation 5 is the theoretical upper limit of the transverse resistivity when a high contact resistance exists between the superconducting filaments and the copper matrix. The volume fraction of the superconducting

filaments, λ, is calculated by equation 6, where r_o is the outer radius of the superconducting strand, r_i is the radius of the bundle of superconducting filaments in the strand, and R is the ratio of the amount of copper matrix material to the amount of superconducting material in the superconductor sample. The matrix resistivity, ρ_m,

$$\lambda = (r_o/r_i)^2/(1+R) \tag{6}$$

is a measured parameter and Fig. 15 and 16 show the measured matrix resistivity of the Nb_3Al samples and the NbTi sample, respectively. The matrix resistivity of the Nb_3Al samples varies as a function of the background magnetic field according to equation 7 for background magnetic fields between zero and two tesla and according to equation 8 for background magnetic fields between two and eight tesla.

$$\rho_m = 0.8 + 0.6B \qquad 0\,T \leq B \leq 2\,T \tag{7}$$

$$\rho_m = 1.07 + 0.465B \qquad 2\,T < B \leq 8\,T \tag{8}$$

The matrix resistivity of the NbTi sample varies as a function of the background magnetic field according to equation 9 for magnetic fields

$$\rho_m = 1.86 + 0.47B \qquad 0\,T \leq B \leq 11\,T \tag{9}$$

between zero and eleven tesla. Finally, the limits of the effective matrix resistivity are calculated by equation 10 [1], where ρ_t is given by equation 5 for the lower time constant limit and equation 4 for the upper time constant limit, and ρ_m is given by equations 7 and 8 for the Nb_3Al samples and equation 9 for the NbTi sample.

$$\frac{1}{\rho_{et}} = \frac{1}{\rho_t} + \frac{(r_o-r_i)}{r_i\rho_m} + \frac{(r_o-r_i)(r_i)}{\rho_m}\left(\frac{2\pi}{L}\right)^2 \tag{10}$$

4.1.2 The Effective Permeability

The effective permeability of the superconducting filaments, μ_{ef}, is calculated by equation 11, where $\mu_o = 4\pi \times 10^{-7}$ second-ohm/meter, λ is the volume fraction of the superconducting filaments as given by

$$\mu_{ef} = \mu_o(1-\alpha\lambda)/(1+\alpha\lambda) \tag{11}$$

equation 6, and m is a parameter that depends on the fraction, η, of the superconducting filament penetrated by the background magnetic field. α is calculated by equation 12 and n is calculated by equations 13 and 14, which are derived from the Bean Model for a superconducting slab [6] Equation 13 is used for background magnetic fields less than $B^*$and

$$\alpha = (1-\eta)/(1+\eta) \tag{12}$$

$$\eta = 0.5B/B^* \qquad 0 \leq B \leq B^* \tag{13}$$

$$\eta = 1 - 0.5(B^*/B) \qquad B^* < B \tag{14}$$

equation 14 is used for background magnetic fields greater than B^*. B^* is the background magnetic field that penetrates exactly to the center of the superconducting filament and is calculated by equation 15, where J_c is the critical current density of the superconductor in

$$B^* = J_c \mu_o r_o \tag{15}$$

a zero background magnetic field and is found from the measured critical currents of the superconductors. Figs. 17 and 18 show the measured critical current densities of the Nb_3Al and NbTi samples, respectively. The critical current densities of the Nb_3Al and NbTi samples in zero background magnetic field are 3.4×10^9 amp-meter^{-2} and 5.6×10^9 amp-meter^{-2}, respectively.

4.2 Theoretical and Measured Time Constant Value Comparison

Figures 19 through 23 show a comparison between the measured time constant values and the theoretical limits of these values. Line (a) of the theoretical limits is the value of the time constants when the effective transverse resistivity, ρ_{et}, of the copper matrix varies with the background magnetic field and the effective permeability, μ_{ef} of the superconducting filaments is considered to remain constant at $4\pi \times 10^{-7}$ second-ohm/meter. Line (b) of the theoretical limits is the value of the time constants when both ρ_{et} and μ_{ef} vary with the background magnetic field. In every superconducting sample, the measured time constant values fell within the theoretical limits.

In the case that μ_{ef} is considered to remain constant (line(a)), the theoretical time constant limits show a smooth decrease in value as the background magnetic field increases. In every superconducting sample

tested, the measured time constant values also decrease as the background magnetic field increases. Although a small amount of fluctuation is present in the decrease of the measured time constant values, this can be attributed to the experimental accuracy of the measurement. Also, for the Nb_3Al samples, the time constant values are not discernably closer to the theoretical maximum or minimum time constant limits. This indicates that the Nb_3Al samples do not approach the limit of a zero contact resistance between the superconducting filaments and the copper matrix nor do they approach the limit of a high contact resistance between the superconducting filaments and the copper matrix. For the NbTi sample, the time constant values are noticeably closer to the minimum time constant limit, which indicates that the NbTi sample approaches the limit of a high contact resistance between the superconducting filaments and the copper matrix.

In the case that μ_{ef} is considered to vary with the background magnetic field according to the Bean Model assumption (line(b)), the theoretical limits show a sharp peak at a low background magnetic field. The theoretical peak occurs at 0.277 tesla for the Nb_3Al samples and at 0.32 tesla for the NbTi sample. This peak also occurs in the measured time constant values of the 10 mm and 30 mm twist pitch Nb_3Al samples at approximately 0.2 tesla, which indicates that the Bean Model for a superconducting slab is a good approximation of the dependence of u_{ef} on the background magnetic field. Although, further testing should be done at background magnetic fields in the area of the peak in order to more precisely verify the Bean Model assumption. The NbTi and the 15 mm and 40 mm twist pitch Nb_3Al samples do not reveal a sharp peak in their measured time constant values at a low background magnetic field. For these samples, no time constant measurements were taken between zero and 0.4 tesla, where the peak is expected to occur. Therefore, a peak which might exist for these samples, could not have been detected.

Figure 24 shows a comparison of the measured time constant values of the four Nb_3Al samples which reveals another correlation between the measured time constant values and the theoretical predictions. The general equation used to calculate the theoretical time constant values, equation 3, predicts that the time constants are proportional to the square of the twist pitch of the superconducting filaments. Fig. 19 reveals a good agreement with this prediction where the time constant values increase for each Nb_3Al sample approximately according to the square of the twist pitch.

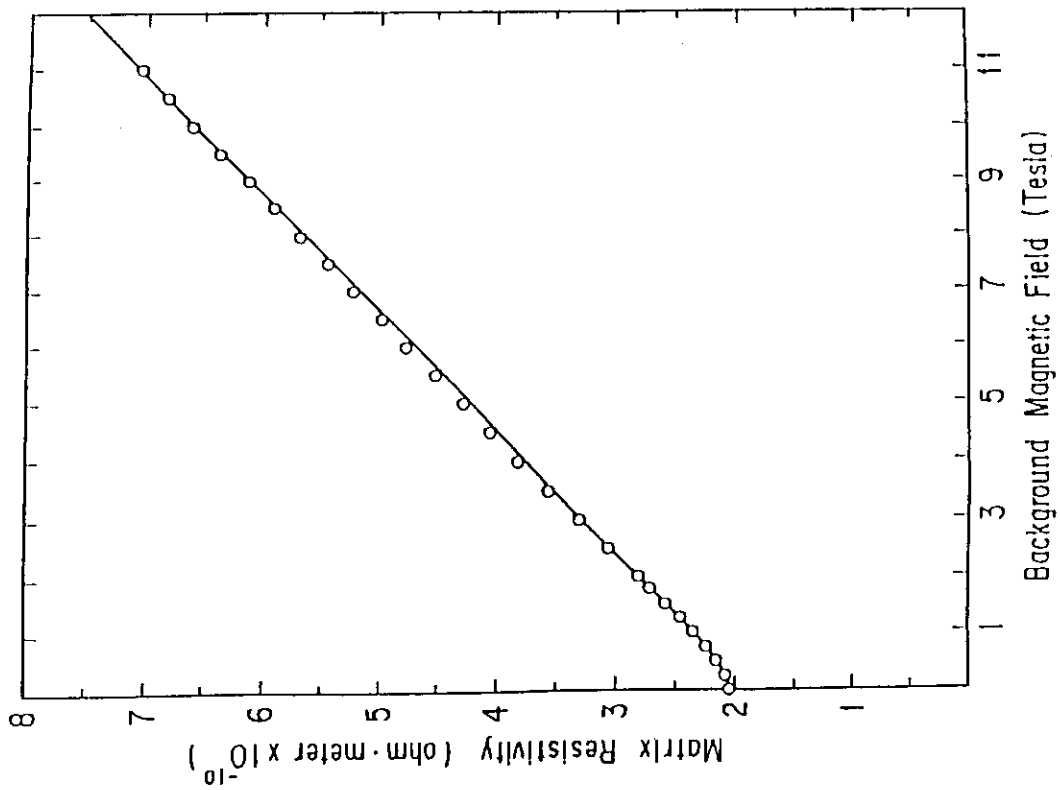

Fig. 15 The measured copper matrix resistivity of the Nb_3Al superconductor.

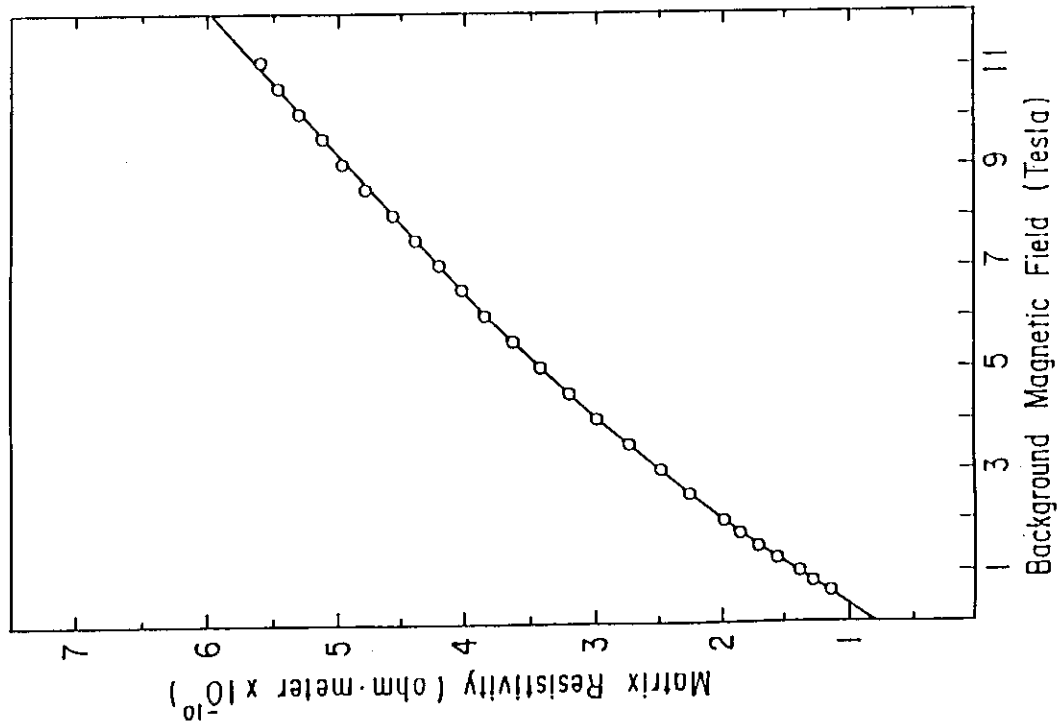

Fig. 16 The measured copper matrix resistivity of the NbTi superconductor.

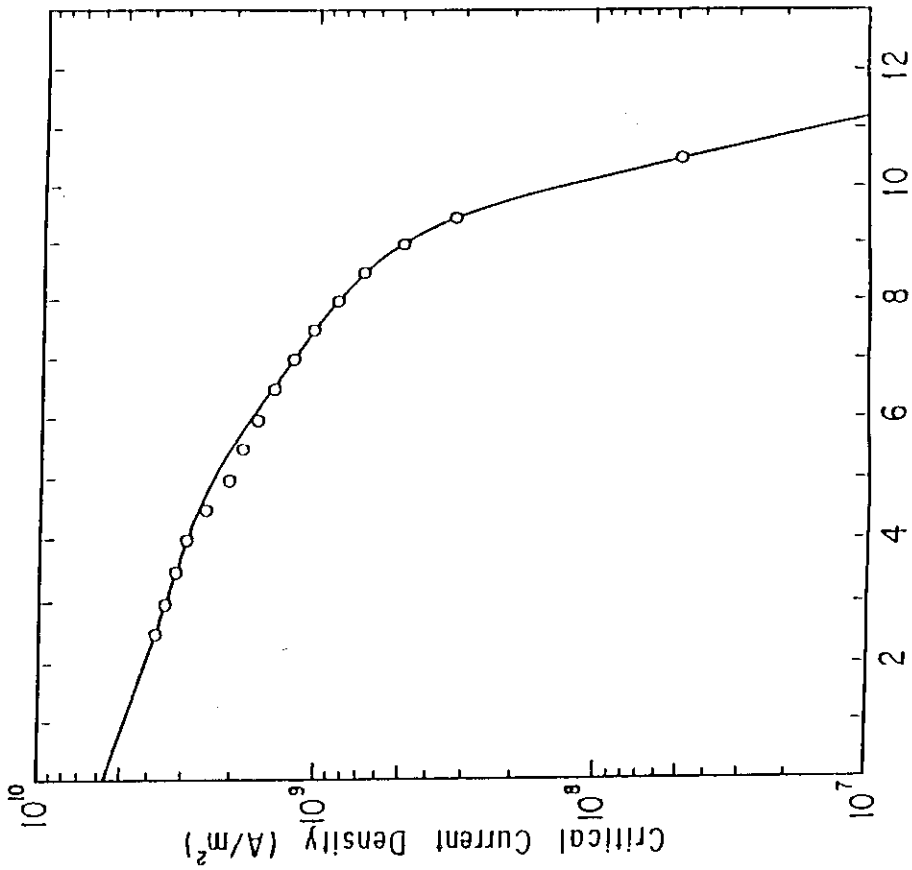

Fig. 17 The measured critical current of the Nb_3Al superconductor.

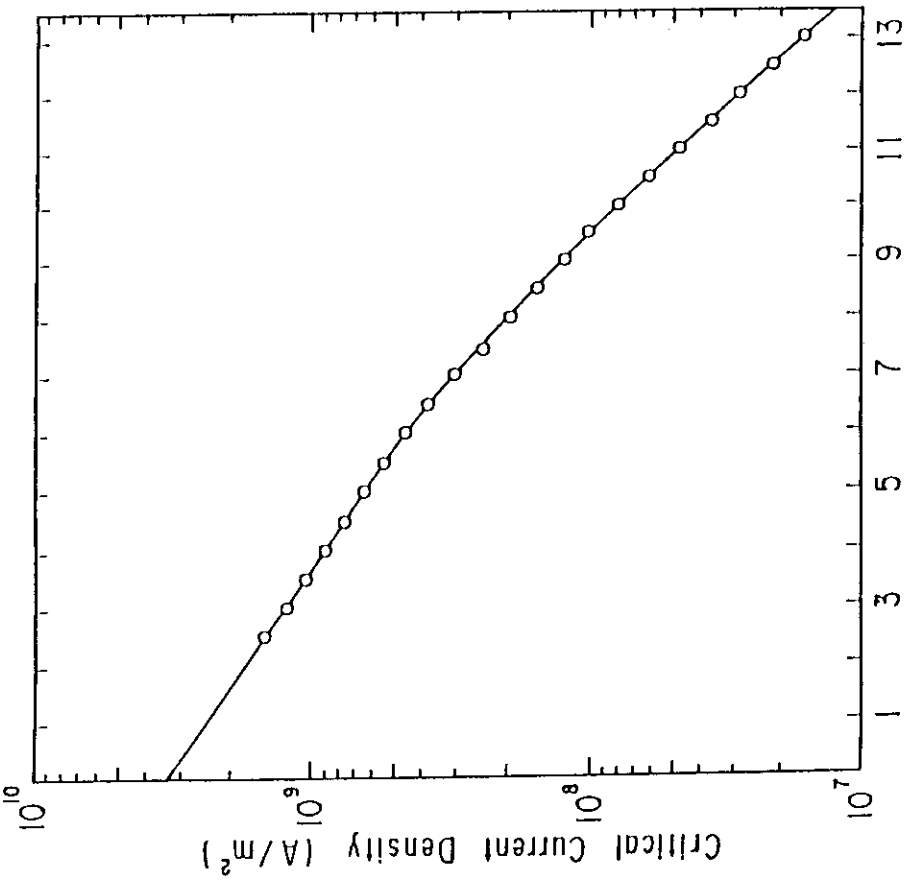

Fig. 18 The measured critical current of the NbTi superconductor.

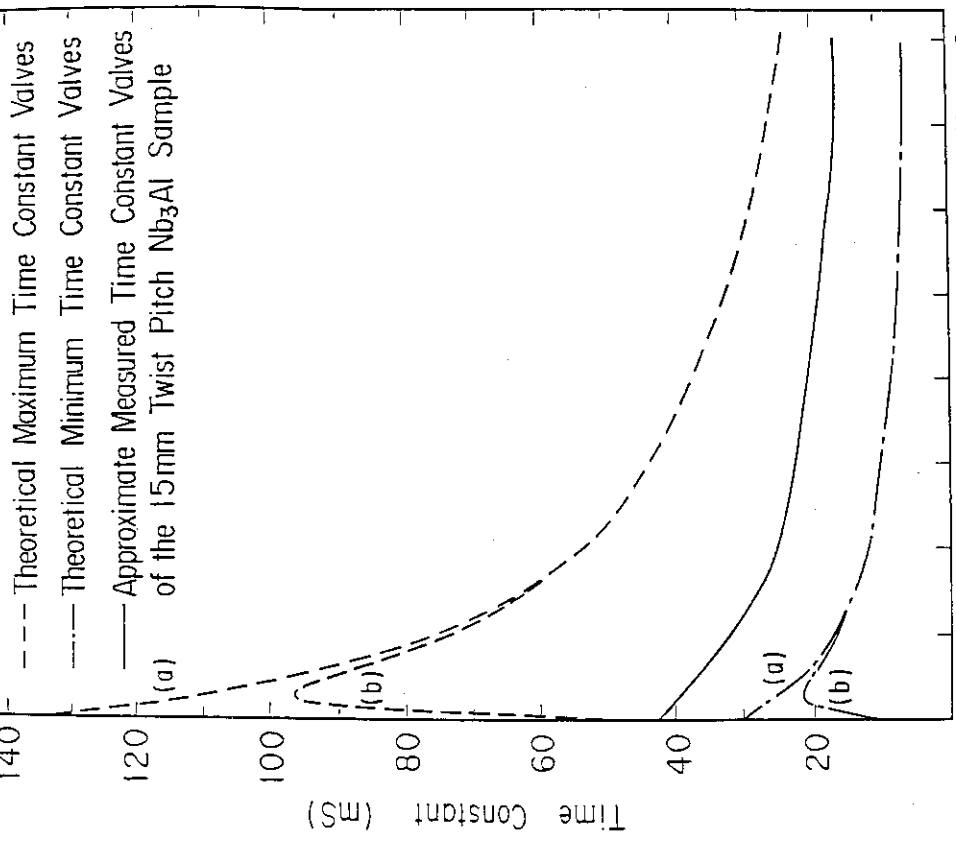

Fig. 20 A comparison of the measured time constant values and their theoretical limits for the 15 mm twist pitch Nb_3Al sample. Line (a) is the theoretical limit when u_{ef} is considered to remain constant, and line (b) is the theoretical limit when u_{ef} is varied.

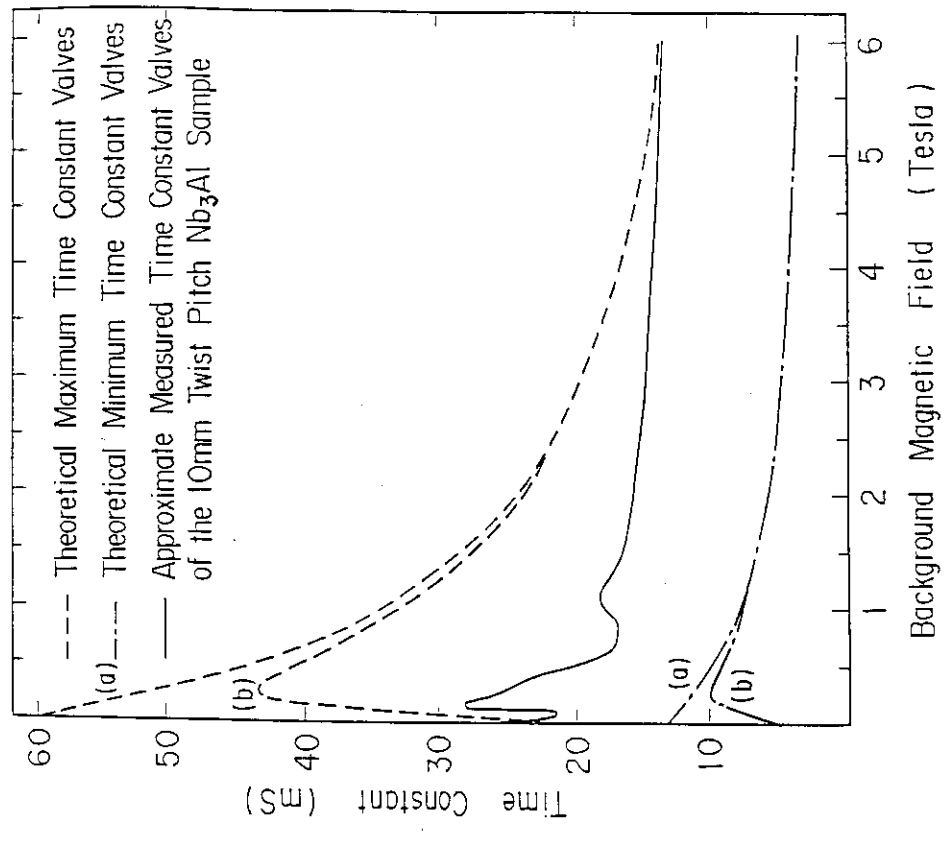

Fig. 19 A comparison of the measured time constant values and their theoretical limits for the 10 mm twist pitch Nb_3Al sample. Line (a) is the theoretical limit when u_{ef} is considered to remain constant, and line (b) is the theoretical limit when u_{ef} is varied.

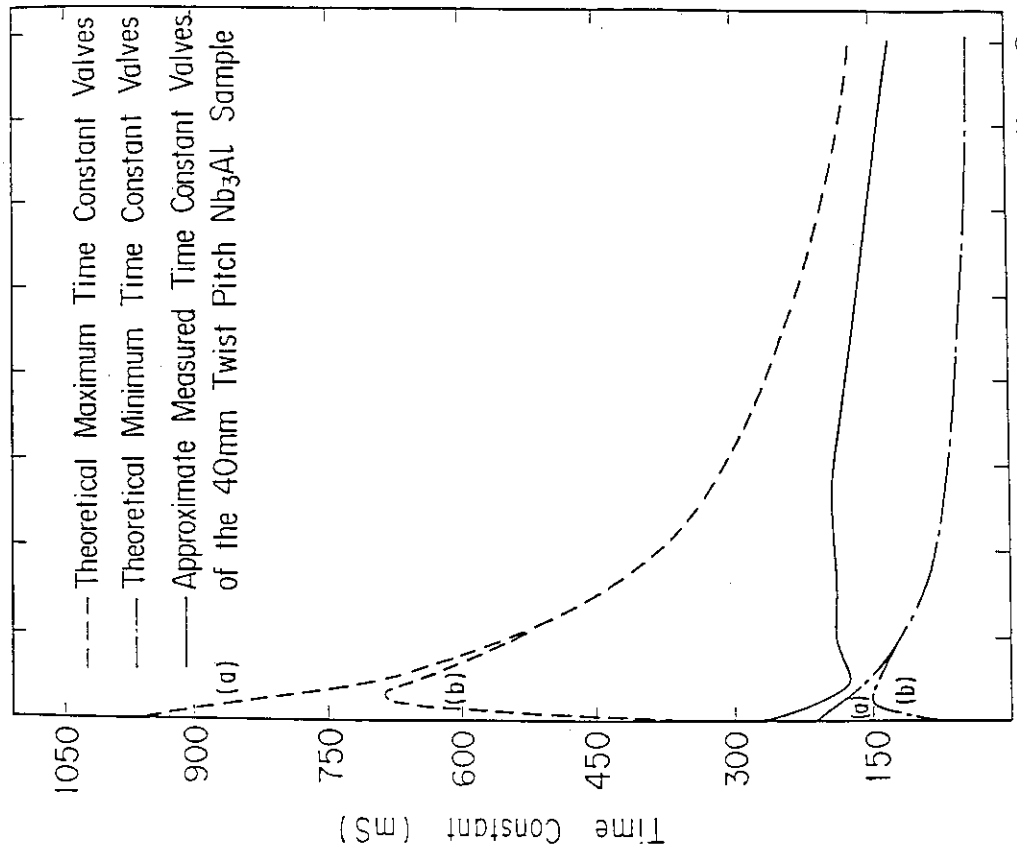

Fig. 22 A comparison of the measured time constant values and their theoretical limits for the 40 mm twist pitch Nb3Al sample. Line (a) is the theoretical limit when u_{ef} is considered to remain constant, and line (b) is the theoretical limit when u_{ef} is varied.

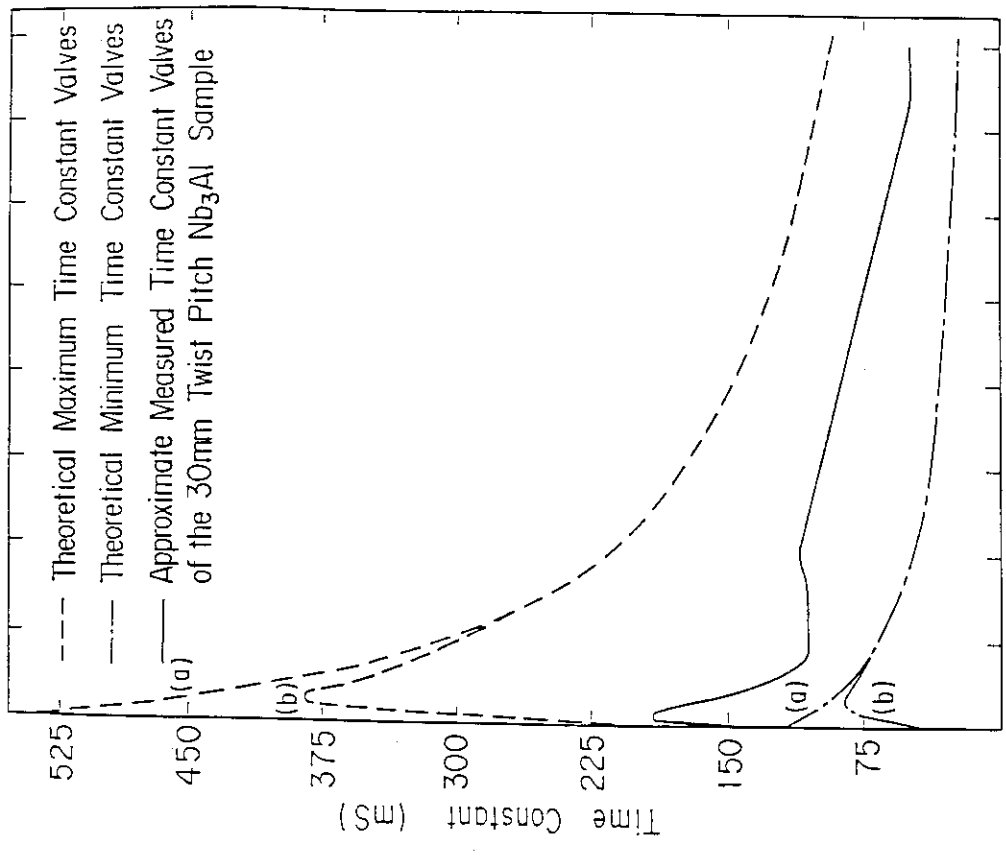

Fig. 21 A comparison of the measured time constant values and their theoretical limits for the 30 mm twist pitch Nb3Al sample. Line (a) is the theoretical limit when u_{ef} is considered to remain constant, and line (b) is the theoretical limit when u_{ef} is varied.

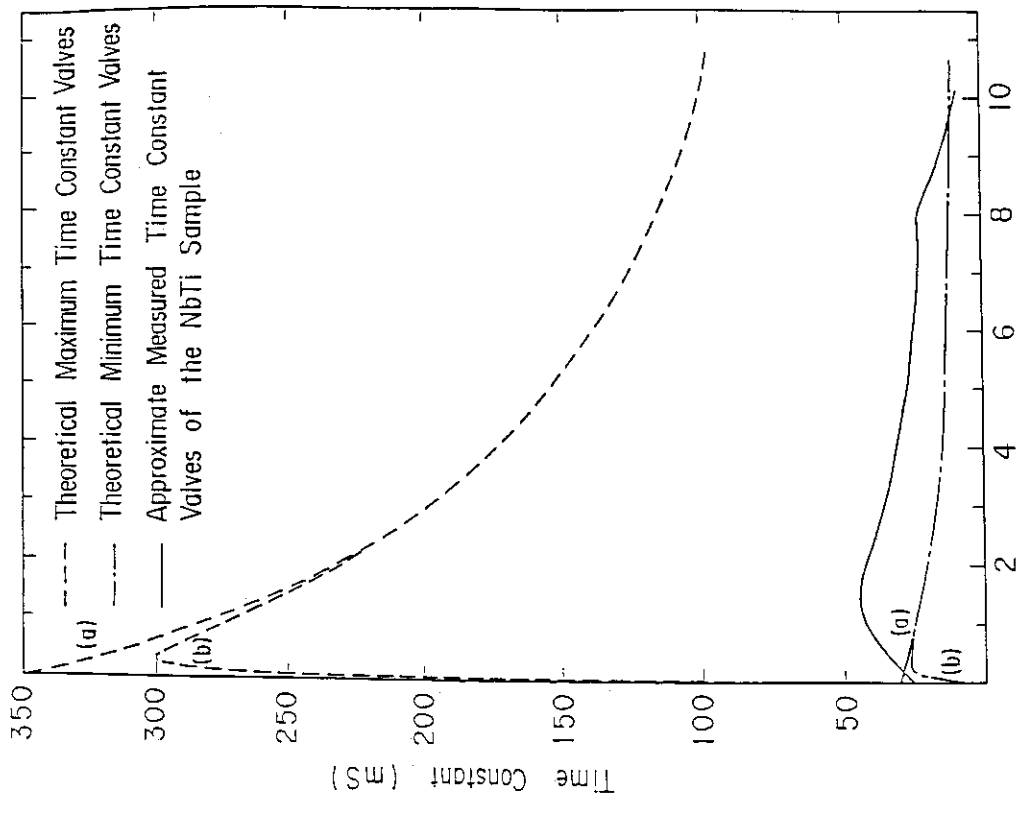

Fig. 23 A comparison of the measured time constrant values and their theoretical limits for the NbTi sample. Line (a) is the theoretical limit when u_{ef} is considered to remain constant, and line (b) is the theoretical limit when u_{ef} is varied.

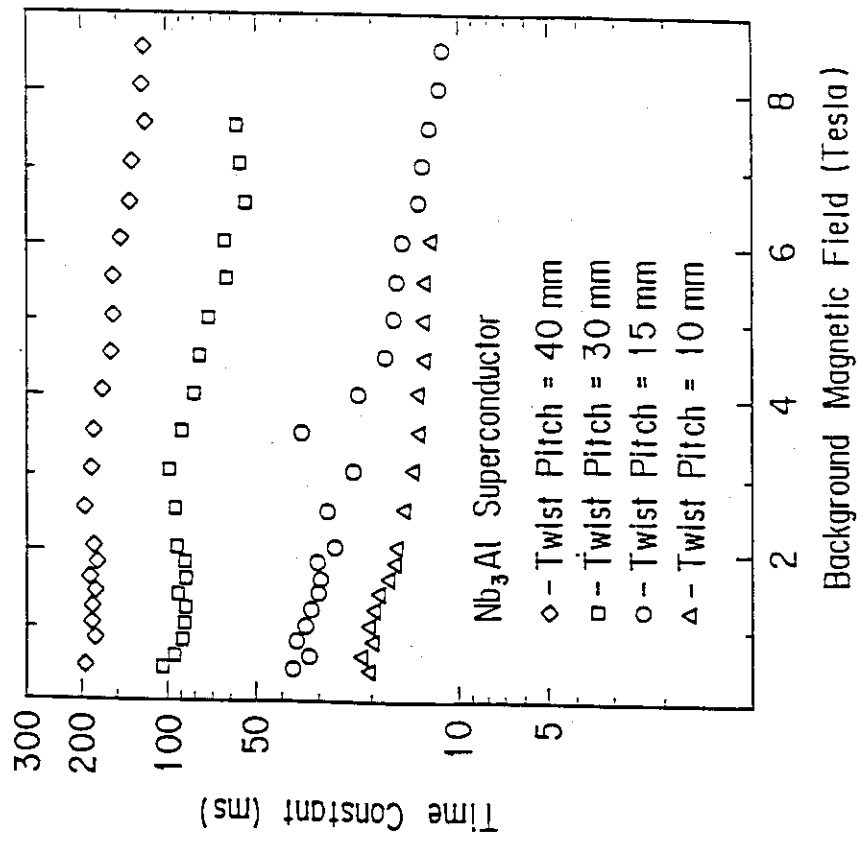

Fig. 24 A comparison of the measured time constants of all the Nb_3Al samples.

5. Conclusions and Recommendations

The conclusions resulting from this investigation are as follows:

The contact resistance between the superconducting filaments and the copper matrix in the multifilamentary Nb3Al superconductor does not approach the theoretical limit of zero resistance or the theoretical limit of a very high resistance, but remains approximately halfway between the two limits.

The contact resistance between the superconducting filaments and the copper matrix in the multifilamentary NbTi superconductor is close to the theoretical limit of a very high resistance.

The variance of the permeability of the Nb3Al superconducting filaments in a background magnetic field is adequately accounted for by the Bean Model for a superconducting slab.

The AC loss time constants of the multifilamentary Nb3Al superconductors vary approximately proportional to the square of the twist pitch of their superconducting filaments.

The recommendation resulting from this investigation is as follows:

A recommended area of future investigation is to study the variance of the AC loss time constants at low background magnetic fields in the area of the peak predicted by the Bean Model for a superconducting slab.

Acknowledgements

My study in Japan would not have been possible without the efforts of Shimamoto Susumu and Yuki Iwasa, who gave me an excellent opportunity to experience the Japanese culture as well as further my education in the superconducting field. Many people have contributed to making my stay in Japan very enjoyable, especially the following: Ando Toshinari, who was my advisor and teacher throughout the experimentation and who gave me excellent knowledge of the superconducting field, Tsuji Hiroshi, who always solved my unsolvable problems, Koizumi Koichi, who showed me most of Kyoto and Nara, Takahashi Yoshikazu and Kawano Katsumi, who both bave me the ability to journey the highways of Japan, Yoshida Kiyoshi, who presented me with the essentials needed for experimenting and everyday living, and the rest of the members of the superconducting magnet laboratory who contributed to my well-being in a variety of ways, Hiyama Tadao, Hoshino Masahiro, Kato Takashi, Nakajima Hideo, Nishi Masataka, Ohgane Yasuo, Okuno Kiyoshi, Oshikiri Masayuki, Satou Masahiko, Tada Eisaku, and Yamamura Hidemasa.

5. Conclusions and Recommendations

The conclusions resulting from this investigation are as follows:

The contact resistance between the superconducting filaments and the copper matrix in the multifilamentary Nb_3Al superconductor does not approach the theoretical limit of zero resistance or the theoretical limit of a very high resistance, but remains approximately halfway between the two limits.

The contact resistance between the superconducting filaments and the copper matrix in the multifilamentary NbTi superconductor is close to the theoretical limit of a very high resistance.

The variance of the permeability of the Nb_3Al superconducting filaments in a background magnetic field is adequately accounted for by the Bean Model for a superconducting slab.

The AC loss time constants of the multifilamentary Nb_3Al superconductors vary approximately proportional to the square of the twist pitch of their superconducting filaments.

The recommendation resulting from this investigation is as follows:

A recommended area of future investigation is to study the variance of the AC loss time constants at low background magnetic fields in the area of the peak predicted by the Bean Model for a superconducting slab.

Acknowledgements

My study in Japan would not have been possible without the efforts of Shimamoto Susumu and Yuki Iwasa, who gave me an excellent opportunity to experience the Japanese culture as well as further my education in the superconducting field. Many people have contributed to making my stay in Japan very enjoyable, especially the following: Ando Toshinari, who was my advisor and teacher throughout the experimentation and who gave me excellent knowledge of the superconducting field, Tsuji Hiroshi, who always solved my unsolvable problems, Koizumi Koichi, who showed me most of Kyoto and Nara, Takahashi Yoshikazu and Kawano Katsumi, who both bave me the ability to journey the highways of Japan, Yoshida Kiyoshi, who presented me with the essentials needed for experimenting and everyday living, and the rest of the members of the superconducting magnet laboratory who contributed to my well-being in a variety of ways, Hiyama Tadao, Hoshino Masahiro, Kato Takashi, Nakajima Hideo, Nishi Masataka, Ohgane Yasuo, Okuno Kiyoshi, Oshikiri Masayuki, Satou Masahiko, Tada Eisaku, and Yamamura Hidemasa.

References

[1] M.N. Wilson, Superconducting Magnets, Oxford University Press, New York, 1983.

[2] J.W. Ekin, "Strain Effects in Superconducting Compounds", Advances in Cryogenic Engineering Materials, Vol. 30, pp823-836.

[3] E. Gregory, "Multifilamentary Superconducting Materials for Large Scale Applications", Cryogenics, May 1982, pp203-212.

[4] T. Ando, Y. Takahashi, M. Nishi, and S. Shimamoto, "Time Constant Measurement Technique for Multifilamentary Superconductors in Parallel Field", Proceedings of International Symposium on Flux Pinning and Electromagnetic Properties in Superconductors, Fukuoka, Japan, November 1985, pp167-170.

[5] W.J. Carr Jr., Journal of Applied Physics, 45 2 (1974) 929.

[6] W.J. Carr, Jr., AC Loss and Macroscopic Theory of Superconductors, Gordon and Breach Science Publishers, Inc., New York, NY, 1983.

[7] T. Ando, Y. Takahashi, M. Nishi, and S. Shimamoto, "AC Losses in a Ta Barrier $Nb_3(SnIn)$ Strand in Demo Poloidal Coil", Presented at The Cryogenic Engineering Conference, Illinois, 1987.

[8] F. Irie, F. Sumiyoshi, and K. Yoshida, "Magnetic Field Dependence of Loss-Frequency Characteristics of Multi-Filamentary Superconductors", IEEE Transactions on Magnetics, Vol. Mag-15, No. 1, January 1979.

[9] B. Turck, F. Lefevre, M. Polak, and L. Krempasky, "Coupling Losses in a Rectangular Multifilamentary Superconducting Composite", Cryogenics, September 1982, pp441-450.

[10] A.M. Campbell, "A general Treatment of Losses in Multifilamentary Superconductors", Cryogenics, January 1982, pp3-16.